Published in final edited form as:
Cell Rep. 2017 December 12; 21(11): 3102–3115. doi:10.1016/j.celrep.2017.11.066.

"Genetic identification of mechanoinsensitive 'silent' nociceptors"

Vincenzo Prato[#1], **Francisco J. Taberner**[#1,2], **James R.F. Hockley**[3], **Gerard Callejo**[3], **Alice Arcourt**[1], **Bassim Tazir**[1], **Leoni Hammer**[1], **Paulina Schad**[1], **Paul A. Heppenstall**[2], **Ewan St. John Smith**[3], and **Stefan G. Lechner**[1,4,*]

[1]Institute of Pharmacology, Heidelberg University, Im Neuenheimer Feld 366, 69120 Heidelberg, Germany

[2]EMBL Monterotondo, Via Ramarini 32, 00016 Monterotondo, Italy

[3]Department of Pharmacology, University of Cambridge, Tennis Court Road, CB2 1PD, United Kingdom

[#] These authors contributed equally to this work.

Summary

Mechanical and thermal hyperalgesia (pain hypersensitivity) are cardinal signs of inflammation. While the mechanism underlying thermal hyperalgesia is well understood, the cellular and molecular basis of mechanical hyperalgesia is poorly described. Here we have identified a subset of peptidergic C-fiber nociceptors that are insensitive to noxious mechanical stimuli under normal conditions, but become sensitized to such stimuli when exposed to the inflammatory mediator nerve growth factor (NGF). Strikingly, NGF did not affect mechanosensitivity of other nociceptors. We show that these mechanoinsensitive 'silent' nociceptors are characterized by the expression of the nicotinic acetylcholine receptor subunit alpha-3 (CHRNA3) and that the mechanically-gated ion channel PIEZO2 mediates NGF-induced mechanosensitivity in these neurons. Retrograde tracing revealed that CHRNA3^{+} nociceptors account for ~50% of all peptidergic nociceptive afferents innervating visceral organs and deep somatic tissues. Hence, our data suggests that NGF-induced 'un-silencing' of CHRNA3^{+} nociceptors significantly contributes to the development of mechanical hyperalgesia during inflammation.

Introduction

The somatosensory nervous system comprises a remarkable variety of neurochemically and functionally diverse sensory afferents that enable us to detect and discriminate a wide range of tactile and noxious stimuli (Dubin and Patapoutian, 2010; Lechner and Lewin, 2013). Sensory neurons that are activated by noxious stimuli are termed nociceptors and are

[*]Correspondence: stefan.lechner@pharma.uni-heidelberg.de.
[4]Lead Contact

The authors declare no conflict of interest.

Author Contributions

Conceptualization, S.G.L.; Methodology, E.St.J.S and S.G.L.; Investigation, V.P., F.J.T., J.R.F.H., G.C., B.T., A.A., L.H. and P.S.; Writing, S.G.L.; Funding Acquisition, E.St.J.S, P.A.H. and S.G.L.; Resources, S.G.L.; Supervision, E.St.J.S, P.A.H. and S.G.L.

Europe PMC Funders Author Manuscripts

subclassified into unmyelinated C-fiber nociceptors and myelinated A-fiber nociceptors. The vast majority of all nociceptors are sensitive to mechanical stimuli, but various subpopulations with different sensitivities to additional noxious stimuli have been described in a wide variety of species. Nociceptors that are exclusively activated by mechanical stimuli are termed C-fiber and A-fiber mechanonociceptors; those that additionally respond to noxious thermal stimuli are collectively termed polymodal nociceptors, but can be further sub-classified according to their specific sensitivity to noxious heat and/or cold (Dubin and Patapoutian, 2010; Lewin and Moshourab, 2004).

The contribution of the various nociceptor subpopulations to different forms of acute pain is quite well understood. C-fibre nociceptors that express the heat-gated ion channel TRPV1, for example, are required for the detection of noxious heat and for the development of heat hyperalgesia (increased pain sensitivity to heat) (Brenneis et al., 2013; Caterina et al., 2000; Cavanaugh et al., 2009) and one study also implicates $TRPV1^+$ afferents in the detection of noxious pinch stimuli (Brenneis et al., 2013). Moreover, it has been shown that noxious cold is detected by C-fibre nociceptors that express the cold and menthol sensitive ion channel TRPM8 (Knowlton et al., 2013). Lastly, whereas noxious mechanical stimuli applied with a blunt probe, such as a von Frey hair, are detected by C-fiber nociceptors that express the Mas-related G-protein coupled receptor D (Cavanaugh et al., 2009), sharp and potentially tissue damaging mechanical stimuli, such as a pinprick, are detected by a subset of A-fibre mechanonociceptors that are characterized by the expression of the neuropeptide Y receptor type 2 (Arcourt et al., 2017).

However, one subpopulation of nociceptors – the so-called ‘silent’ nociceptors – has remained enigmatic ever since it had first been described (Gold and Gebhart, 2010; Michaelis et al., 1996). The term silent nociceptor was originally introduced to describe sensory afferents that fired action potentials in response to electrical stimulation of the receptive field, but could not be activated by physiologically relevant noxious mechanical stimuli. Silent nociceptors have been found in large numbers in the urinary bladder, the distal colon and the knee joint (Feng and Gebhart, 2011; Gebhart, 1999; Häbler et al., 1990; Schaible and Schmidt, 1988), but are rare in rodent skin (Wetzel et al., 2007). In the human skin, however, silent afferents account for almost one quarter of all C-fibre nociceptors (Schmidt et al., 1995). The fact that silent nociceptors are normally not activated by mechanical stimuli, suggests that they are not involved in mechanical pain signalling in healthy individuals. However, several studies have shown that silent afferents are sensitized to mechanical stimuli by a variety of compounds that are commonly used to experimentally induce inflammation, as well as by endogenous inflammatory mediators such as nerve growth factor (NGF) (Feng et al., 2012; Gold and Gebhart, 2010; Hirth et al., 2013; Schaible and Schmidt, 1985). Considering the large proportion of mechanically insensitive afferents in the above-mentioned tissues, it is conceivable that un-silencing them would greatly increase nociceptive input to pain processing circuits in the spinal cord and higher brain regions. Accordingly it has been proposed that silent afferents may significantly contribute to mechanical hyperalgesia during inflammation (Gold and Gebhart, 2010). However, owing to the lack of molecular markers that would allow the unequivocal identification or the selective functional manipulation of silent afferents, this hypothesis has never been directly

tested. Moreover, the molecular mechanism that mediates the un-silencing of silent nociceptors has not yet been described.

Results

CHRNA3$^+$ sensory neurons are mechanoinsensitive peptidergic C-fibre nociceptors

Mechanosensitivity of dorsal root ganglion (DRG) sensory neurons is usually examined with the patch-clamp technique by recording whole-cell transmembrane currents evoked by mechanical stimulation of the cell soma (Figure 1A). In DRG neurons three types of mechanically-activated currents, which differ in their inactivation kinetics and were thus termed rapidly-adapting (RA), intermediately-adapting (IA) and slowly-adapting (SA) currents, have been described (Drew et al., 2002; Hu and Lewin, 2006; McCarter et al., 1999; Ranade et al., 2014). The ion channel PIEZO2 mediates the RA-current in low-threshold mechanoreceptors (LTMRs), which detect tactile stimuli, but the mechanically-gated channel required for mechanotransduction in nociceptors is still unknown (Ranade et al., 2014; Schrenk-Siemens et al., 2015). While we were screening several reporter mouse lines with the original goal to test if IA- and SA-currents are confined to genetically defined subsets of nociceptors, we made the observation that neurons in which EGFP is expressed under the control of the promoter of the nicotinic acetylcholine receptor subunit alpha-3 (CHRNA3) do not respond to mechanical stimuli at all. Thus only 1 from 15 tested CHRNA3$^+$ cells exhibited a tiny inward current in response to mechanical stimulation of the soma (Figure 1B-D). By contrast, the majority of peptidergic C-fibre nociceptors (27 from 32 tested neurons), non-peptidergic nociceptors (13 from 17) and LTMRs (18 from 21) exhibited large mechanically-evoked inward currents (Figure 1B-D), which was consistent with previously published data (Drew et al., 2002; Hu and Lewin, 2006; Ranade et al., 2014). In these recordings, LTMRs and nociceptors were distinguished by means of cell size as well as action potential (AP) shape and duration, as previously described (Fang et al., 2005; Koerber et al., 1988). Peptidergic and non-peptidergic nociceptors were further discriminated by isolectin B4 (IB4) labeling, which specifically binds to non-peptidergic nociceptors (Figure 1E) (Molliver et al., 1997). Thus, small diameter IB4-neg neurons with wide APs that exhibited the nociceptor specific hump in the falling phase were classified as peptidergic C-fibre nociceptors and large diameter neurons with narrow uninflected spikes were classified as LTMRs (Figure 1E-G). CHRNA3$^+$ neurons exhibited APs that were indistinguishable from those of other nociceptors but were significantly different from the action potentials of LTMRs (Figure 1F and G). Moreover, CHRNA3$^+$ neurons were not labeled by IB4 (Figure 1E), had small to medium size cell bodies and accounted for 7.8 ± 1.6 % (n=636) of the total population in cultures of L2-L5 DRGs (Figure 1H). To test if CHRNA3$^+$ neurons – as suggested by their AP configuration – are indeed nociceptors, we next examined the expression of well-established nociceptor subpopulation markers in CHRNA3$^+$ neurons in L3-L5 DRGs (Figure 2A–D). The great majority of CHRNA3$^+$ neurons expressed the NGF receptor TRKA (94.6 ± 4.1 %, Figure 2A and 2D) and the calcitonin gene-related peptide (CGRP; 90.5 ± 2.5 %, Figure 2C and 2D), which are markers for peptidergic nociceptors (Averill et al., 1995), but did not express the GDNF receptor RET (1.8 ± 3.0 %, Figure 2B and 2D), which is present in non-peptidergic neurons (Molliver et al., 1997). Moreover, only a few CHRNA3$^+$ neurons showed immunoreactivity for

neurofilament heavy polypeptide (NEFH) (11.6 ± 5.4 %, Figure 2A and 2D), which is only expressed in myelinated sensory neurons. The central projections of CHRNA3$^+$ neurons predominantly terminated in lamina I of the dorsal horn of the spinal cord, which is also characteristic of peptidergic nociceptors (Figure 2E) (Braz et al., 2014). We also observed EGFP immunoreactivity in local neurons in lamina IIo of the dorsal horn and scattered throughout lamina III. However, unlike the EGFP signals in lamina I, the signals in deeper laminae did not overlap with CGRP immunofluorescence (see insets in Figure 2E) and thus unlikely originate from CHRNA3$^+$ sensory afferents. Hence the electrophysiological data together with the immunohistochemical analysis strongly suggests that CHRNA3$^+$ neurons are mechanically insensitive, ‘silent’, peptidergic C-fibre nociceptors.

CHRNA3$^+$ neurons densely innervate deep somatic tissues and viscera but are absent from the skin

Silent nociceptors have originally not only been found in the knee joint (Schaible and Schmidt, 1985), which is innervated by L3-L4 DRG neurons that we had investigated so far, but were shown to be even more abundant in visceral organs (Michaelis et al., 1996). Hence we next examined CHRNA3 expression in other spinal segments. Indeed CHRNA3$^+$ neurons were present in all DRGs from cervical (C1) to sacral (S1) and almost all of them expressed CGRP (Figure 2F and Figure S1A). More importantly, this analysis revealed that CHRNA3$^+$ neurons are rather rare in most DRGs (~15% of all CGRP$^+$ neurons) but account for up to 40% of the CGRP$^+$ population in thoracolumbar (T12-L1) and lumbosacral (L6-S1) DRGs (Figure 2F and 2G). This finding strongly supports our hypothesis that CHRNA3$^+$ neurons are silent nociceptors, because these DRGs give rise to the lumbar splanchnic nerve and the pelvic nerve, which innervate the colon and the bladder where silent afferent have been found in large numbers (Christianson et al., 2007; Michaelis et al., 1996). While analyzing the immunolabeled sections, we noticed the presence of numerous neurons with an extremely bright GFP fluorescence in lumbosacral DRGs (Figure 2F and S1B). Indeed the GFP intensity distributions in L6-S1 DRGs and in T12-L1 DRGs were best fit with the sum of two Gaussians, whereas they were better fitted with a single Gaussian in all other DRGs, suggesting that two different populations of CHRNA3$^+$ neurons that significantly differ in their GFP intensities (hereafter termed GFP^{low} and GFP^{high} neurons) are present in thoracolumbar and lumbosacral DRGs (Figure S1C). GFP^{low} neurons had significantly higher levels of CGRP when compared to GFP^{high} neurons (Figure S1D), suggesting that these two populations may also differ in their functional properties. To test this hypothesis we examined mechanosensitivity of the two populations in various spinal segments. GFP^{low} neurons from all spinal segments as well as GFP^{high} neurons from the thoracolumbar region were insensitive to mechanical stimuli, whereas GFP^{high} neurons from lumbosacral DRGs exhibited large mechanotransduction currents (Figure S2A and S2B). Hence unless otherwise stated, hereafter the term “CHRNA3$^+$ neurons” refers to the mechanoinsensitive GFP^{low} population.

We next examined the peripheral projections of CHRNA3$^+$ neurons (Figure 3A-F). In the distal colon and the urinary bladder, CHRNA3$^+$ fibres accounted for 92.1 ± 0.8 % and 81.1 ± 0.5 % of all CGRP$^+$ fibres, respectively (Figure 3B, C and F). Moreover we observed numerous CHRNA3$^+$ afferents in the knee joint (63.2 ± 0.7 % of CGRP$^+$ fibres, Figure 3D

and F) and the gastrocnemius muscle (62.5 ± 2.3% of $CGRP^+$ fibres, Figure 3E and F), but we did not find any $CHRNA3^+$ fibres in the glabrous and hairy skin (Figure 3A and Figure S3A). Some sympathetic neurons, which also innervate the examined tissues, also expressed CHRNA3. However, these cells did not express CGRP (Figure S3B-S2C), supporting the hypothesis that the $CHRNA3^+/CGRP^+$ fibres shown in Figure 3B-E indeed originate from $CHRNA3^+$ sensory neurons. Heterogeneity in the GFP intensities, as observed in DRG stainings (Figure 2F and S1B-C), was not evident in stainings of the bladder and the colon. Hence, to clarify whether the observed $CHRNA3^+$ fibres originated from GFP^{low} or GFP^{high} neurons we next labeled sensory neurons that innervate the bladder and the colon with the retrograde tracer fast blue (FB, Figure 4A-B). In T13 DRGs, 39.1 ± 3.2 % of the $CGRP^+$ neurons that innervate the colon were GFP^{low} while less than 10% were GFP^{high}. By contrast in S1 DRGs, both GFP^{low} (55 ± 6 % of FB+/CGRP+ neurons) and GFP^{high} (37.2 ± 14.4 %) neurons were labeled by fast blue injection into the colon (Figure 4A, D and E). Similar results were obtained for the bladder, where FB injection labeled both GFP^{low} (40.5 ± 4.9 %) and GFP^{high} (41.2 ± 0.7 %) neurons in S1 DRGs, but almost exclusively GFP^{low} cells (36.1 ± 12.7 %) in T13 DRGs (Figure 4B and 4F). We also labeled knee joint afferents, which predominantly originate from L3 and L4 DRGs (da Silva Serra et al., 2016). Consistent with our previous results (Figure 3F), 56.2 ± 15.4 % and 42.1 ± 10.7 % of the $FB^+/CGRP^+$ neurons in L4 and L3 DRGs, respectively, were CHRNA3 positive (Figure 4C and G).

Hence taken together, our data demonstrates that mechanoinsensitive $CHRNA3^+$ sensory neurons account for approximately half of all peptidergic nociceptors in tissues previously shown to be densely innervated by silent afferents (Feng and Gebhart, 2011; Gebhart, 1999; Häbler et al., 1990; Schaible and Schmidt, 1988).

$CHRNA3^+$ neurons are sensitized to mechanical stimuli by NGF

A key feature of silent nociceptors is their ability to become sensitized to mechanical stimuli by inflammatory mediators. We thus next asked if $CHRNA3^+$ (GFP^{low} from L2-L5 DRGs) neurons acquire mechanosensitivity after treatment with NGF (50 ng/ml) or an inflammatory soup containing 10 μM bradykinin, 10 μM prostaglandin E_2, 10 μM histamine and 10 μM serotonin. One-hour treatment with NGF or the inflammatory soup did not affect mechanosensitivity of $CHRNA3^+$ neurons (Figure 5A-C; note that both treatments were applied after the cells had been cultured in normal growth medium for 24 hours). After 24 hours treatment with NGF, however, $CHRNA3^+$ neurons acquired mechanosensitivity and responded to mechanical stimulation with large inward currents, which did not further increase when NGF and inflammatory soup were applied together (Figure 5A-C). Interestingly, NGF did not modulate the amplitude or the kinetics of mechanotransduction currents in small diameter IB4-neg neurons – i.e. putative TRKA-expressing peptidergic C-fiber nociceptors (Figure 5D-F). Inflammatory soup alone also had no effect on mechanosensitivity of IB4-neg neurons. However, after 24 hours treatment with NGF, 1-hour treatment with the inflammatory soup caused a small, but significant increase of mechanotransduction current amplitudes elicited by small membrane displacements (Figure 5E), as well as a slowing of inactivation kinetics (Figure 5F).

Via binding to the TRKA receptor, NGF can activate multiple signaling pathways including the PLCγ pathway, the PI3-Kinase pathway and the Ras/Raf/MEK/ERK pathway (Bibel and Barde, 2000). To examine which of these signaling pathways mediated the sensitization of CHRNA3$^+$ neurons we next incubated DRG cultures for 24 hours with NGF in the presence of either 5 μM U73122, a PLCγ blocker, 500 nM wortmannin (WTM), a PI3-kinase blocker, or 10 μM U0126 an ERK1/2 blocker (Figure 6A). U73122 and wortmannin did not alter the effect of NGF treatment, but CHRNA3$^+$ neurons treated with U0126 exhibited significantly smaller mechanotransduction currents than neurons from the same cultures treated with NGF alone (Figure 6B). ERK1/2 kinases can regulate gene transcription, but can also directly modulate ion channels by phosphorylation. To test if the former mechanism is involved, we incubated CHRNA3$^+$ neurons for 24 hours with NGF in the presence of the transcription blocker actinomycin D (2 μg/ml). Indeed mechanotransduction currents were significantly smaller when cultures were treated with actinomycin D (Figure 6B), suggesting that de-novo gene transcription is required for the NGF-induced acquisition of mechanosensitivity in CHRNA3$^+$ neurons.

We next sought to identify the ion channel that confers mechanosensitivity on CHRNA3$^+$ neurons. In LTMRs, RA-type mechanotransduction currents are mediated by PIEZO2, but the ion channel that mediates mechanotransduction currents in nociceptors is still unknown (Ranade et al., 2014). Several proteins have been implicated in mechanosensitivity of sensory neurons such as the acid-sensing ion channels ASIC2 and ASIC3 (Price et al., 2000, 2001), the transient receptor potential channels TRPA1 (Vilceanu and Stucky, 2010), TRPC3 and TRPC6 (Quick et al., 2012) and TMEM150c (Hong et al., 2016), but conflicting results have been published regarding their precise role in mechanotransduction (Drew et al., 2004; Dubin et al., 2017). To test if any of these putative mechanotransduction genes was present in CHRNA3$^+$ neurons and up-regulated by NGF, we next compared their mRNA levels in CHRNA3$^+$ neurons from L2-L5 DRGs cultured for 24 hours in the presence and absence of NGF using qPCR (Figure 7A). This analysis showed that transcripts for none of these proteins were up-regulated by NGF. Unexpectedly however, the qPCR data revealed that – even under control conditions – CHRNA3$^+$ neurons express PIEZO2 at levels comparable to those in LTMRs. The presence of PIEZO2 was further confirmed by immunolabeling of L2-L5 DRGs, which showed that 94.9 % (278/293) of the CHRNA3$^+$ neurons express PIEZO2 (Figure 7B), suggesting that mechanotransduction currents in CHRNA3$^+$ neurons are indeed mediated by PIEZO2. This hypothesis was supported by additional electrophysiological experiments showing that – similar to PIEZO2-mediated currents (Coste et al., 2010) – mechanotransduction currents in CHRNA3$^+$ neurons reversed at close to 0 mV and exhibited significantly slower inactivation kinetics at positive membrane potentials (Figure 7C-E). Moreover, mechanotransduction currents in CHRNA3$^+$ neurons were inhibited by the toxin GsMTx4 (Figure 7F), which had been shown to block PIEZO2 currents (Wang et al., 2017). Finally, siRNA-mediated knockdown of PIEZO2 expression in CHRNA3$^+$ neurons prevented the acquisition of mechanosensitivity in NGF treated cells (Figure 7G and H).

In summary, our data shows that PIEZO2 confers mechanosensitivity to CHRNA3$^+$ neurons. However, since PIEZO2 is also expressed in the absence of NGF – i.e. under conditions in which CHRNA3$^+$ neurons do not exhibit mechanotransduction currents – our data further

suggests that PIEZO2 is normally inhibited in these cells and is released from this inhibition by NGF-induced up-regulation of a yet unidentified protein (Figure 7I).

Discussion

Here, we have identified a molecular marker for mechanoinsensitive 'silent' nociceptors. We show that sensory neurons that express CHRNA3 constitute a subset of peptidergic C-fibre nociceptors that are completely insensitive to mechanical stimuli under normal conditions, but become sensitized to such stimuli when exposed to the inflammatory mediator NGF. Strikingly, mechanosensitivity of other nociceptors does not appear to be affected by NGF treatment. We further show that the mechanically-gated ion channel PIEZO2 mediates NGF-induced mechanosensitivity in CHRNA3$^+$ nociceptors. Since CHRNA3$^+$ afferents account for ~50% of all peptidergic nociceptors innervating visceral organs and deep somatic tissues, we propose that the NGF-induced un-silencing of CHRNA3$^+$ afferents significantly contributes to the development of mechanical hyperalgesia during inflammation.

The contribution of CHRNA3$^+$ neurons to inflammation-induced mechanical hyperalgesia

NGF plays an important role in the induction and maintenance of pain hypersensitivity associated with inflammation (Denk et al., 2017; Lewin et al., 2014), which is highlighted by several important observations. Thus a single NGF injection induces profound and long-lasting thermal and mechanical hyperalgesia in rodents and humans (Dyck et al., 1997; Lewin et al., 1993; Rukwied et al., 2010). Moreover, sequestering endogenously produced NGF with anti-NGF antibodies blocks hyperalgesia associated with experimentally induced inflammation in rodents (Woolf et al., 1994) and – most importantly – alleviates pain in humans suffering from a variety of painful chronic inflammatory diseases (Chang et al., 2016; Denk et al., 2017). While the mechanism underlying NGF-induced heat hyperalgesia is well understood, only little is known about the cellular and molecular basis of mechanical hyperalgesia.

Our data suggests that CHRNA3$^+$ silent nociceptors may contribute to the development of inflammatory mechanical hyperalgesia in visceral organs, muscles and joints, via the following mechanism: under normal conditions CHRNA3$^+$ neurons are mechanoinsensitive (Figure 1A-D) and hence noxious mechanical stimuli only activate other – mechanosensitive – nociceptors leading to normal pain perception (Figure 7I). During inflammation however, increased NGF levels in the inflamed tissues (Chen et al., 2016; Denk et al., 2017; Iannone et al., 2002; di Mola et al., 2000) lead to un-silencing of CHRNA3$^+$ afferents (Figure 5A-C). Considering that silent afferents account for ~50% of all nociceptors in these tissues (Figure 4), the consequence of this un-silencing is that the number of nociceptive afferents that are activated by a given noxious mechanical stimulus is doubled, which inevitably results in significantly increased excitatory drive onto projection neurons in the spinal cord and hence to increased pain sensitivity (Figure 7I).

So is this model in accordance with previously published data and models regarding possible mechanisms of mechanical hyperalgesia? First, we would like to emphasize that we do not claim that the un-silencing of CHRNA3$^+$ afferent is the only mechanism underlying NGF-induced hyperalgesia. Our findings do not rule out a possible contribution of previously

described mechanisms such as NGF-induced increases in the synthesis and release of brain-derived neurotrophic factor (BDNF) from the central synapses of nociceptors, which leads to strengthened synaptic transmission and hence amplified pain signaling, or NGF-induced changes in the electrical excitability of nociceptors resulting from subtle changes in the expression levels and the functional properties of the voltage-gated sodium channels Nav1.7 and Nav1.8 (Lewin et al., 2014; Pezet and McMahon, 2006). However, given the remarkable sensitivity to NGF (Figure 5) and the high incidence of CHRNA3^{+} afferents in viscera and deep somatic tissues (Figure 3 and 4), it is tempting to speculate that the contribution of CHRNA3^{+} afferents to pain hypersensitivity in these tissues is quite considerable. Indeed there is compelling clinical evidence indicating that NGF-signaling plays a particularly important role in the development of pain hypersensitivity in the joints, in the bladder and in muscles. Thus numerous clinical trials have demonstrated that anti-NGF therapy shows particularly great efficacy in alleviating pain associated with osteoarthritis, interstitial cystitis and low back pain (Chang et al., 2016; Denk et al., 2017). Our observation that mechanoinsensitive CHRNA3^{+} afferents account for approximately 50 % of all peptidergic nociceptors in the colon, the bladder, the knee joint and in muscles (Figure 3 and 4) is consistent with previous electrophysiological studies, which found that the proportion of silent afferents among C-fibre nociceptors is between 30 and 90 % in these tissues (Feng and Gebhart, 2011; Gebhart, 1999; Gold and Gebhart, 2010; Häbler et al., 1990; Michaelis et al., 1996; Schaible and Schmidt, 1985). Silent afferents have also been found in large numbers (~ 25%) in cutaneous nerves of humans and monkeys (Meyer et al., 1991; Schmidt et al., 1995), but they appear to be extremely rare (< 10 % of all C-fibre nociceptors) in the mouse skin (Wetzel et al., 2007). Hence, the absence of CHRNA3^{+} afferents from both hairy and glabrous skin (Figure 3A and S3A) was not fully unexpected. It is unlikely that we overlooked CHRNA3^{+} afferents innervating the skin, considering that we have analyzed a total of 120 skin sections from three different mice. Hence, we propose that silent cutaneous afferents are genetically different from those innervating the viscera and deep somatic tissues.

The effects of NGF on mechanosensitivity

Another important finding of our study was that NGF only sensitizes CHRNA3^{+} neurons, but not other TRKA-expressing nociceptors (IB4^{neg} neurons), to mechanical stimuli (Figure 5). At first glance the finding that IB4^{neg} neurons are not sensitized to mechanical stimuli appears to contradict previous reports from others and us, showing that mechanotransduction currents in IB4^{neg} neurons are modulated by NGF (Di Castro et al., 2006; Lechner et al., 2009). In this context, it is important to note that here we have used adult animals (8-12 weeks old), whereas in our previous study we have examined neurons from newborn mice (Lechner et al., 2009) and di Castro and colleagues (2006) have studied juvenile rats. However, it is well known that NGF is important for the functional maturation of sensory neurons during embryonic and postnatal development of sensory neurons (Lewin et al., 2014; Luo et al., 2007). We have actually shown that NGF is required for the developmental acquisition of mechanosensitivity in IB4^{neg} neurons (Lechner et al., 2009). Moreover, it was shown that the diversification of nociceptors into peptidergic TRKA^{+} neurons and non-peptidergic TRKA^{-}/RET^{+} neurons is only completed three weeks after birth (Bennett et al., 1996; Molliver and Snider, 1997; Molliver et al., 1997). Hence NGF-dependent effects

observed in newborn or juvenile animals should be interpreted with caution as they might solely reflect incomplete maturation of nociceptors. Indeed using extracellular single-unit recordings from the saphenous nerve it was recently shown that in the complete Freund's adjuvant (CFA) model of inflammation, peripheral sensitization of cutaneous nociceptors only occurs in young but not in aged mice (Weyer et al., 2016). So does that mean that mechanosensitivity of CHRNA3-neg peptidergic nociceptors is not at all altered during inflammation and that NGF does in general not modulate the functional properties of these neurons? Not quite. Although our data shows that NGF does not directly modulate mechanotransduction currents in $IB4^{neg}$ neurons, we demonstrate that an inflammatory soup only potentiates mechanotransduction currents after pretreatment with NGF (Figure 5E). A possible explanation for this observation is that NGF up-regulates the expression of genes that are required for the actions of other inflammatory mediators. Indeed it has been shown that the B2 receptor for bradykinin, which was present in the inflammatory soup used in this study, is upregulated in nociceptors by NGF (Lee et al., 2002). Moreover di Castro et al. (2006) showed that – in juvenile rats – direct activation of protein kinase C with the phorbol ester PMA only sensitizes mechanotransduction currents in $IB4^{neg}$ neurons after pretreatment with NGF. Hence, we conclude that in addition to inducing a complete phenotypic switch in $CHRNA3^{+}$ neurons, NGF primes other peptidergic nociceptors for subsequent sensitization by other inflammatory mediators, which however only have moderate effects on mechanosensitivity.

The molecular basis of NGF-induced mechanosensitivity in $CHRNA3^{+}$ neurons

During the last two decades numerous ion channels, such as ASIC channels, TRPA1, TRPC3, TRPC6, TMEM150c and PIEZO2 have been proposed to contribute to mechanosensitivity of sensory neurons (Hong et al., 2016; Price et al., 2000, 2001; Quick et al., 2012; Ranade et al., 2014; Vilceanu and Stucky, 2010). However, conflicting results have been published regarding the precise role of some of these channels in mechanotransduction (Drew et al., 2004; Dubin et al., 2017). The only channel that has convincingly been shown to be required for mechanosensitivity of sensory neurons is PIEZO2. First, unlike the other above-mentioned channels, PIEZO2 alone is sufficient to produce mechanotransduction currents when expressed in heterologous systems (Coste et al., 2010). Moreover, PIEZO2 knock-out mice have severe deficits in proprioception (Woo et al., 2015) and in gentle touch perception (Ranade et al., 2014 Interestingly, PIEZO2 knock-out mice do not seem to have problems with detecting noxious mechanical stimuli and do develop hyperalgesia in the paw skin in the CFA model of inflammation (Ranade et al., 2014). However, PIEZO2 is expressed in almost 50% of all sensory neurons (Ranade et al., 2014), some of which express the heat-gated ion channel TRPV1 (Coste et al., 2010), suggesting that PIEZO2 is also present in some nociceptors. Using qPCR and immunohistochemistry, we show that PIEZO2 is indeed expressed in some nociceptors, namely in $CHRNA3^{+}$ neurons (Figure 7A and B). Moreover, the current-voltage relationship together with the voltage-dependence of the inactivation kinetics and the GsMTX4-sensitivity (Figure 7C-F), and – most importantly – the observation that siRNA-mediated knockdown of PIEZO2 renders NGF-treated $CHRNA3^{+}$ neurons insensitive to mechanical stimuli (Figure 7G and H), suggests that the NGF-induced mechanotransduction currents in $CHRNA3^{+}$ neurons are indeed mediated by PIEZO2. So why is it that PIEZO2 knock-out mice do not have a pain phenotype? The

simple answer is that Ranade et al (2014) only examined cutaneous nociceptors, but as our data demonstrates, CHRNA3$^+$ afferents do not innervate the skin. An important question that, however, remains open is why CHRNA3$^+$ neurons are insensitive to mechanical stimuli under control conditions even though they express PIEZO2 (Figure 7A and B)? At present we can only speculate about the possible mechanism. Our experiments, however, demonstrate that de-novo gene transcription is required for the acquisition of mechanosensitivity (Figure 6A and B). Hence, as illustrated in Figure 7I, we propose that PIEZO2 is normally inhibited by a yet unknown protein and is released from this inhibition by another unidentified protein that is upregulated by NGF-TRKA-ERK1/2 signaling.

Conclusions

NGF signaling plays a central role in the development of mechanical hyperalgesia associated with inflammation. Despite the great efficacy of anti-NGF antibodies in alleviating pain, however, in 2010 all anti-NGF trials were placed on clinical hold for a period of almost five years, due to a high incidence of joint destruction in osteoarthritis patients receiving anti-NGF treatment and concerns regarding possible side effects on sympathetic neurons (Chang et al., 2016; Denk et al., 2017). Our work, especially the identification of a nociceptor subpopulation that is particularly sensitive to NGF and that predominantly innervates tissues in which anti-NGF therapy has proven extremely efficacious, provides an invaluable framework for future studies that aim to further unravel the mechanism underlying NGF-induced hyperalgesia and studies that aim at developing drugs that selectively block the effects of NGF in sensory neurons and would thus potentially have fewer side effects than currently available anti-NGF drugs.

Experimental Procedures

Animals

CHRNA3-EGFP mice, official name Tg(Chrna3-EGFP)BZ135Gsat/Mmnc (RRID:MMRRC_000243-UNC) were obtained from the Mutant Mouse Resource & Research Center (MMRRC) and were backcrossed to a C57Bl/6J background. Additional information is provided in the Supplemental Experimental Procedures.

Immunohistochemistry

A detailed description of the immunostaining protocols and the antibodies that were used is provided in the Supplemental Experimental Procedures.

Cell culture

8-12 weeks old mice were killed by placing them in a CO_2-filled chamber for 2–4 min followed by cervical dislocation and DRGs were collected in Ca^{2+} and Mg^{2+}-free PBS. DRGs were subsequently treated with collagenase IV for 30 minutes (1 mg/ml, Sigma) and with trypsin (0.05 %, Life Technologies) for a further 30 minutes, at 37 °C. Digested DRG's were washed twice with growth medium [DMEM-F12 (Invitrogen) supplemented with L-glutamine (2 μM, Sigma), glucose (8 mg/ml, Sigma), penicillin (200 U/ml)–streptomycin (200 μg/ml) (both Life Technologies) 5 % fetal horse serum (Life Technologies)], triturated using fire-polished Pasteur pipettes and plated in a droplet of growth medium on a glass

coverslip precoated with poly-L-lysine (20 μg/cm^2, Sigma) and laminin (4μg/cm^2, Life Technologies). To allow neurons to adhere, coverslips were kept for 3 - 4 hours at 37 °C in a humidified 5 % incubator before being flooded with fresh growth medium. Cultures were used for patch-clamp experiments on the next day.

Patch-clamp recordings

Whole cell patch clamp recordings were made at room temperature (20-24°C) with an EPC10 amplifier (HEKA, Lambrecht, Germany) and patch pipettes with a resistance of 2-4 MΩ. The intracellular solution consisted of 110 mM KCl, 10 mM NaCl, 1 mM $MgCl_2$, 1 mM EGTA, 10 mM HEPES, 2 mM guanosine 5'-triphosphate (GTP) and 2 mM adenosine 5'-triphosphate (ATP) adjusted to pH 7.3 with KOH. The bathing solution contained 140 mM NaCl, 4 mM KCl, 2 mM $CaCl_2$, 1 mM $MgCl_2$, 4 mM glucose, 10 mM HEPES, adjusted to pH 7.4 with NaOH. Mechanically activated currents were recorded in the whole-cell patch-clamp configuration. Neurons were clamped to a holding potential of -60 mV and stimulated with a series of mechanical stimuli in 1.6 μm increments with a fire-polished glass pipette (tip diameter 2-3μm) that was positioned at an angle of 45° to the surface of the dish and moved with a velocity of 3.5μm/ms by a piezo-driven micromanipulator (MM3A, Kleindiek Nanotechnik, Reutlingen, Germany). Additional information is provided in the Supplemental Experimental Procedures.

Retrograde labeling

A detailed description of the retrograde labeling procedure is provided in the Supplemental Experimental Procedures.

Single cell electroporation and siRNA-mediated knockdown

CHRNA3$^+$ neurons were transfected with non-targeting siRNA (, D-001810-01-05 ON-TARGETplus Non-targeting siRNA, GE-Healthcare) and PIEZO2-siRNA (L-163012-00-0005 ON-TARGETplus Mouse Piezo2 (667742) siRNA – SMARTpool), respectively, using single cell electroporation. Details about the electroporation procedure are provided in the Supplemental Experimental Procedures.

Reverse transcription and quantitative real-time PCR

mRNA expression levels of candidate mechanotransduction genes in CHRNA3$^+$ neurons were determined from samples containing 20 CHRNA3$^+$ neurons that were collected from DRG cultures by aspirating the cells into a patch clamp pipette filled with 2-4μl PBS containing 4 U/μl RNAseOUT (Thermofisher). cDNA synthesis was carried out directly on the sample using the Power SYBR® Green Cells-to-CT™ Kit (Life Technologies) following the manufacturers instructions. qPCR reactions were performed using FastStart Essential DNA Green Master (Roche) on a LightCycler 96 (Roche). Detailed information about primers and thermal cycle profile is provided in the Supplemental Experimental Procedures.

Supplementary Material

Refer to Web version on PubMed Central for supplementary material.

Achnowledgements

This study was supported by the DFG grants LE3210/1-1 and SFB1158/1 to S.G.L., DFG SFB1158/2 to P.A.H., Arthritis Research UK grant #20930 to G.C. and E.St.J.S. as well as the Rosetrees Trust grant # A1296 to J.R.F.H. and E.St.J.S. We also thank Ms. Anke Niemann for technical assistance.

References

Arcourt A, Gorham L, Dhandapani R, Prato V, Taberner FJ, Wende H, Gangadharan V, Birchmeier C, Heppenstall PA, Lechner SG. Touch Receptor-Derived Sensory Information Alleviates Acute Pain Signaling and Fine-Tunes Nociceptive Reflex Coordination. Neuron. 2017; 93:179–193. [PubMed: 27989460]

Averill S, McMahon SB, Clary DO, Reichardt LF, Priestley JV. Immunocytochemical localization of trkA receptors in chemically identified subgroups of adult rat sensory neurons. Eur J Neurosci. 1995; 7:1484–1494. [PubMed: 7551174]

Bennett DL, Averill S, Clary DO, Priestley JV, McMahon SB. Postnatal changes in the expression of the trkA high-affinity NGF receptor in primary sensory neurons. Eur J Neurosci. 1996; 8:2204–2208. [PubMed: 8921312]

Bibel M, Barde Y. Neurotrophins: key regulators of cell fate and cell shape in the vertebrate nervous system. Genes Dev. 2000; 14:2919–2937. [PubMed: 11114882]

Braz J, Solorzano C, Wang X, Basbaum AI. Transmitting pain and itch messages: a contemporary view of the spinal cord circuits that generate gate control. Neuron. 2014; 82:522–536. [PubMed: 24811377]

Brenneis C, Kistner K, Puopolo M, Segal D, Roberson D, Sisignano M, Labocha S, Ferreirós N, Strominger A, Cobos EJ, et al. Phenotyping the Function of TRPV1-Expressing Sensory Neurons by Targeted Axonal Silencing. J Neurosci. 2013; 33:315–326. [PubMed: 23283344]

Caterina MJ, Leffler A, Malmberg AB, Martin WJ, Trafton J, Petersen-Zeitz KR, Koltzenburg M, Basbaum AI, Julius D. Impaired nociception and pain sensation in mice lacking the capsaicin receptor. Science. 2000; 288:306–313. [PubMed: 10764638]

Cavanaugh DJ, Lee H, Lo L, Shields SD, Zylka MJ, Basbaum AI, Anderson DJ. Distinct subsets of unmyelinated primary sensory fibers mediate behavioral responses to noxious thermal and mechanical stimuli. Proc Natl Acad Sci. 2009; 106:9075–9080. [PubMed: 19451647]

Chang DS, Hsu E, Hottinger DG, Cohen SP. Anti-nerve growth factor in pain management: current evidence. J Pain Res. 2016; 9:373–383. [PubMed: 27354823]

Chen W, Ye D-Y, Han D-J, Fu G-Q, Zeng X, Lin W, Liang Y. Elevated level of nerve growth factor in the bladder pain syndrome/interstitial cystitis: a meta-analysis. SpringerPlus. 2016; 5:1072. [PubMed: 27462520]

Christianson JA, Liang R, Ustinova EE, Davis BM, Fraser MO, Pezzone MA. Convergence of Bladder and Colon Sensory Innervation Occurs at the Primary Afferent Level. Pain. 2007; 128:235–243. [PubMed: 17070995]

Coste B, Mathur J, Schmidt M, Earley TJ, Ranade S, Petrus MJ, Dubin AE, Patapoutian A. Piezo1 and Piezo2 are essential components of distinct mechanically activated cation channels. Science. 2010; 330:55–60. [PubMed: 20813920]

Denk F, Bennett DL, McMahon SB. Nerve Growth Factor and Pain Mechanisms. Annu Rev Neurosci. 2017; 40 null.

Di Castro A, Drew LJ, Wood JN, Cesare P. Modulation of sensory neuron mechanotransduction by PKC- and nerve growth factor-dependent pathways. Proc Natl Acad Sci U S A. 2006; 103:4699–4704. [PubMed: 16537426]

Drew L, Wood J, Cesare P. Distinct mechanosensitive properties of capsaicin-sensitive and -insensitive sensory neurons. J Neurosci Off J Soc Neurosci. 2002; 22:RC228–RC228.

Drew L, Rohrer D, Price M, Blaver K, Cockayne D, Cesare P, Wood J. Acid-sensing ion channels ASIC2 and ASIC3 do not contribute to mechanically activated currents in mammalian sensory neurones. J Physiol. 2004; 556:691–710. [PubMed: 14990679]

Dubin AE, Patapoutian A. Nociceptors: the sensors of the pain pathway. J Clin Invest. 2010; 120:3760–3772. [PubMed: 21041958]

Dubin AE, Murthy S, Lewis AH, Brosse L, Cahalan SM, Grandl J, Coste B, Patapoutian A. Endogenous Piezo1 Can Confound Mechanically Activated Channel Identification and Characterization. Neuron. 2017; 94:266–270.e3. [PubMed: 28426961]

Dyck PJ, Peroutka S, Rask C, Burton E, Baker MK, Lehman KA, Gillen DA, Hokanson JL, O'Brien PC. Intradermal recombinant human nerve growth factor induces pressure allodynia and lowered heat-pain threshold in humans. Neurology. 1997; 48:501–505. [PubMed: 9040746]

Fang X, McMullan S, Lawson SN, Djouhri L. Electrophysiological differences between nociceptive and non-nociceptive dorsal root ganglion neurones in the rat in vivo. J Physiol. 2005; 565:927–943. [PubMed: 15831536]

Feng B, Gebhart GF. Characterization of silent afferents in the pelvic and splanchnic innervations of the mouse colorectum. Am J Physiol Gastrointest Liver Physiol. 2011; 300:G170–80. [PubMed: 21071510]

Feng B, La J-H, Schwartz ES, Tanaka T, McMurray TP, Gebhart GF. Long-term sensitization of mechanosensitive and -insensitive afferents in mice with persistent colorectal hypersensitivity. Am J Physiol Gastrointest Liver Physiol. 2012; 302:G676–683. [PubMed: 22268098]

Gebhart GF. Peripheral contributions to visceral hyperalgesia. Can J Gastroenterol J Can Gastroenterol. 1999; 13(Suppl A):37A–41A.

Gold MS, Gebhart GF. Nociceptor sensitization in pain pathogenesis. Nat Med. 2010; 16:1248–1257. [PubMed: 20948530]

Häbler HJ, Jänig W, Koltzenburg M. Activation of unmyelinated afferent fibres by mechanical stimuli and inflammation of the urinary bladder in the cat. J Physiol. 1990; 425:545–562. [PubMed: 2213588]

Hirth M, Rukwied R, Gromann A, Turnquist B, Weinkauf B, Francke K, Albrecht P, Rice F, Hägglöf B, Ringkamp M, et al. Nerve growth factor induces sensitization of nociceptors without evidence for increased intraepidermal nerve fiber density. Pain. 2013; 154:2500–2511. [PubMed: 23891896]

Hong G-S, Lee B, Wee J, Chun H, Kim H, Jung J, Cha JY, Riew T-R, Kim GH, Kim I-B. Tentonin 3/TMEM150c Confers Distinct Mechanosensitive Currents in Dorsal-Root Ganglion Neurons with Proprioceptive Function. Neuron. 2016; 91:107–118. [PubMed: 27321926]

Hu J, Lewin GR. Mechanosensitive currents in the neurites of cultured mouse sensory neurones. J Physiol. 2006; 577:815–828. [PubMed: 17038434]

Iannone F, De Bari C, Dell'Accio F, Covelli M, Patella V, Lo Bianco G, Lapadula G. Increased expression of nerve growth factor (NGF) and high affinity NGF receptor (p140 TrkA) in human osteoarthritic chondrocytes. Rheumatol Oxf Engl. 2002; 41:1413–1418.

Knowlton WM, Palkar R, Lippoldt EK, McCoy DD, Baluch F, Chen J, McKemy DD. A Sensory-Labeled Line for Cold: TRPM8-Expressing Sensory Neurons Define the Cellular Basis for Cold, Cold Pain, and Cooling-Mediated Analgesia. J Neurosci. 2013; 33:2837–2848. [PubMed: 23407943]

Koerber HR, Druzinsky RE, Mendell LM. Properties of somata of spinal dorsal root ganglion cells differ according to peripheral receptor innervated. J Neurophysiol. 1988; 60:1584–1596. [PubMed: 3199173]

Lechner SG, Lewin GR. Hairy sensation. Physiol Bethesda Md. 2013; 28:142–150.

Lechner SG, Frenzel H, Wang R, Lewin GR. Developmental waves of mechanosensitivity acquisition in sensory neuron subtypes during embryonic development. EMBO J. 2009; 28:1479–1491. [PubMed: 19322198]

Lee Y-J, Zachrisson O, Tonge DA, McNaughton PA. Upregulation of bradykinin B2 receptor expression by neurotrophic factors and nerve injury in mouse sensory neurons. Mol Cell Neurosci. 2002; 19:186–200. [PubMed: 11860272]

Lewin G, Moshourab R. Mechanosensation and pain. J Neurobiol. 2004; 61:30–44. [PubMed: 15362151]

Lewin GR, Ritter AM, Mendell LM. Nerve growth factor-induced hyperalgesia in the neonatal and adult rat. J Neurosci. 1993; 13:2136–2148. [PubMed: 8478693]

Europe PMC Funders Author Manuscripts

Lewin GR, Lechner SG, Smith ESJ. Nerve growth factor and nociception: from experimental embryology to new analgesic therapy. Handb Exp Pharmacol. 2014; 220:251–282. [PubMed: 24668476]

Luo W, Wickramasinghe SR, Savitt JM, Griffin JW, Dawson TM, Ginty DD. A Hierarchical NGF Signaling Cascade Controls Ret-Dependent and Ret-Independent Events during Development of Nonpeptidergic DRG Neurons. Neuron. 2007; 54:739–754. [PubMed: 17553423]

McCarter G, Reichling D, Levine J. Mechanical transduction by rat dorsal root ganglion neurons in vitro. Neurosci Lett. 1999; 273:179–182. [PubMed: 10515188]

Meyer RA, Davis KD, Cohen RH, Treede RD, Campbell JN. Mechanically insensitive afferents (MIAs) in cutaneous nerves of monkey. Brain Res. 1991; 561:252–261. [PubMed: 1802341]

Michaelis M, Häbler HJ, Jäenig W. Silent afferents: a separate class of primary afferents? Clin Exp Pharmacol Physiol. 1996; 23:99–105. [PubMed: 8819636]

di Mola FF, Friess H, Zhu ZW, Koliopanos A, Bley T, Di Sebastiano P, Innocenti P, Zimmermann A, Büchler MW. Nerve growth factor and Trk high affinity receptor (TrkA) gene expression in inflammatory bowel disease. Gut. 2000; 46:670–679. [PubMed: 10764711]

Molliver D, Snider W. Nerve growth factor receptor TrkA is downregulated during postnatal development by a subset of dorsal root ganglion neurons. J Comp Neurol. 1997; 381:428–438. [PubMed: 9136800]

Molliver D, Wright D, Leitner M, Parsadanian A, Doster K, Wen D, Yan Q, Snider W. IB4-binding DRG neurons switch from NGF to GDNF dependence in early postnatal life. Neuron. 1997; 19:849–861. [PubMed: 9354331]

Pezet S, McMahon SB. Neurotrophins: mediators and modulators of pain. Annu Rev Neurosci. 2006; 29:507–538. [PubMed: 16776595]

Price M, Lewin G, McIlwrath S, Cheng C, Xie J, Heppenstall P, Stucky C, Mannsfeldt A, Brennan T, Drummond H, et al. The mammalian sodium channel BNC1 is required for normal touch sensation. Nature. 2000; 407:1007–1011. [PubMed: 11069180]

Price M, McIlwrath S, Xie J, Cheng C, Qiao J, Tarr D, Sluka K, Brennan T, Lewin G, Welsh M. The DRASIC cation channel contributes to the detection of cutaneous touch and acid stimuli in mice. Neuron. 2001; 32:1071–1083. [PubMed: 11754838]

Quick K, Zhao J, Eijkelkamp N, Linley JE, Rugiero F, Cox JJ, Raouf R, Gringhuis M, Sexton JE, Abramowitz J, et al. TRPC3 and TRPC6 are essential for normal mechanotransduction in subsets of sensory neurons and cochlear hair cells. Open Biol. 2012; 2:120068. [PubMed: 22724068]

Ranade SS, Woo S-H, Dubin AE, Moshourab RA, Wetzel C, Petrus M, Mathur J, Bégay V, Coste B, Mainquist J, et al. Piezo2 is the major transducer of mechanical forces for touch sensation in mice. Nature. 2014; 516:121–125. [PubMed: 25471886]

Rukwied R, Mayer A, Kluschina O, Obreja O, Schley M, Schmelz M. NGF induces non-inflammatory localized and lasting mechanical and thermal hypersensitivity in human skin. Pain. 2010; 148:407–413. [PubMed: 20022698]

Schaible H, Schmidt R. Time course of mechanosensitivity changes in articular afferents during a developing experimental arthritis. J Neurophysiol. 1988; 60:2180–2195. [PubMed: 3236065]

Schaible HG, Schmidt RF. Effects of an experimental arthritis on the sensory properties of fine articular afferent units. J Neurophysiol. 1985; 54:1109–1122. [PubMed: 4078610]

Schmidt R, Schmelz M, Forster C, Ringkamp M, Torebjörk E, Handwerker H. Novel classes of responsive and unresponsive C nociceptors in human skin. J Neurosci. 1995; 15:333–341. [PubMed: 7823139]

Schrenk-Siemens K, Wende H, Prato V, Song K, Rostock C, Loewer A, Utikal J, Lewin GR, Lechner SG, Siemens J. PIEZO2 is required for mechanotransduction in human stem cell-derived touch receptors. Nat Neurosci. 2015; 18:10–16. [PubMed: 25469543]

da Silva Serra I, Husson Z, Bartlett JD, Smith ESJ. Characterization of cutaneous and articular sensory neurons. Mol Pain. 2016; 12

Vilceanu D, Stucky CL. TRPA1 Mediates Mechanical Currents in the Plasma Membrane of Mouse Sensory Neurons. PLoS ONE. 2010; 5

Wang F, Knutson K, Alcaino C, Linden DR, Gibbons SJ, Kashyap P, Grover M, Oeckler R, Gottlieb PA, Li HJ, et al. Mechanosensitive ion channel Piezo2 is important for enterochromaffin cell response to mechanical forces. J Physiol. 2017; 595:79–91. [PubMed: 27392819]

Wetzel C, Hu J, Riethmacher D, Benckendorff A, Harder L, Eilers A, Moshourab R, Kozlenkov A, Labuz D, Caspani O, et al. A stomatin-domain protein essential for touch sensation in the mouse. Nature. 2007; 445:206–209. [PubMed: 17167420]

Weyer AD, Zappia KJ, Garrison SR, O'Hara CL, Dodge AK, Stucky CL. Nociceptor Sensitization Depends on Age and Pain Chronicity. eNeuro. 2016; 3

Woo S-H, Lukacs V, de Nooij JC, Zaytseva D, Criddle CR, Francisco A, Jessell TM, Wilkinson KA, Patapoutian A. Piezo2 is the principal mechanotransduction channel for proprioception. Nat Neurosci. 2015; 18:1756–1762. [PubMed: 26551544]

Woolf CJ, Safieh-Garabedian B, Ma QP, Crilly P, Winter J. Nerve growth factor contributes to the generation of inflammatory sensory hypersensitivity. Neuroscience. 1994; 62:327–331. [PubMed: 7530342]

Europe PMC Funders Author Manuscripts

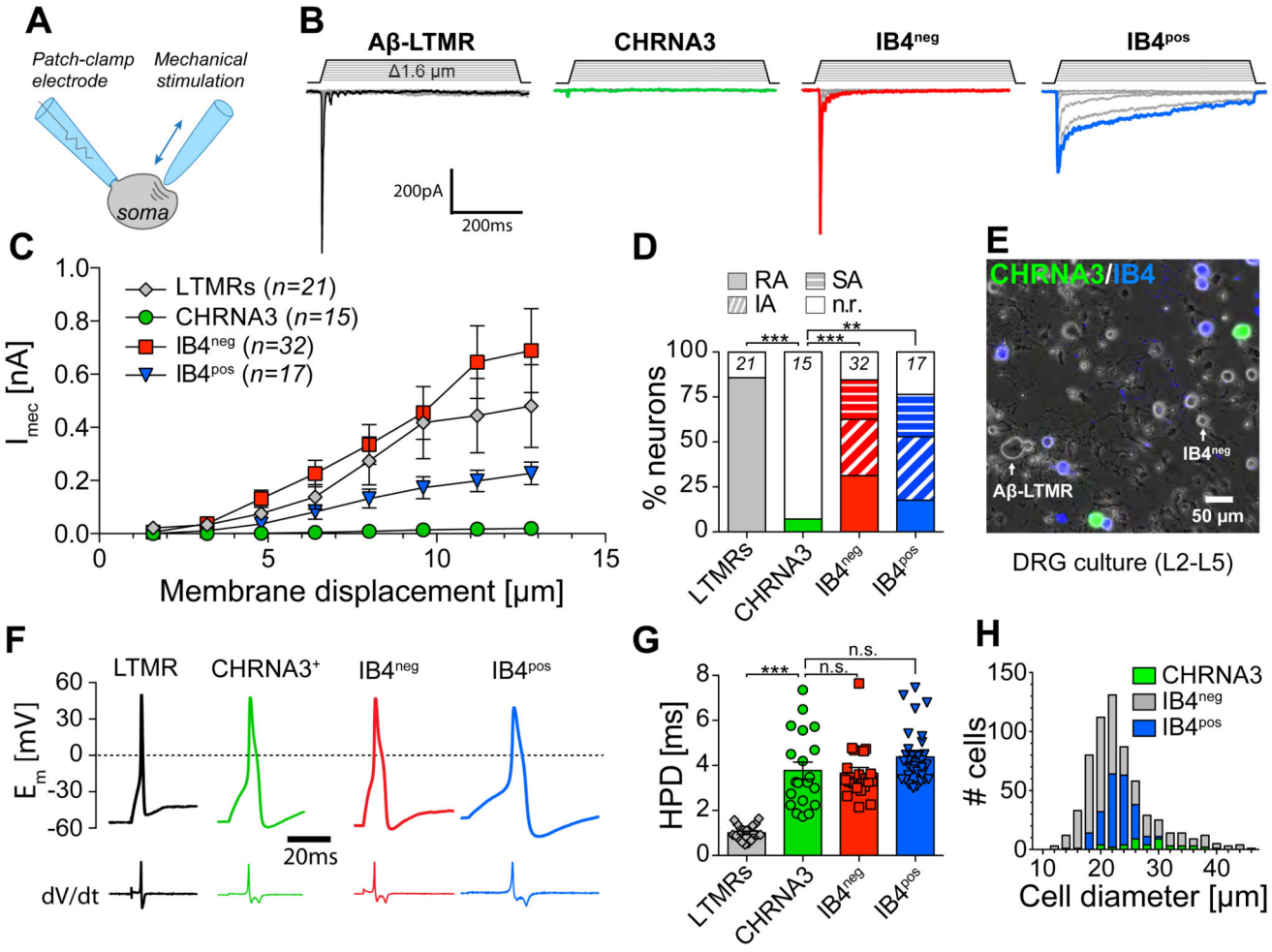

Figure 1. CHRNA3^{+} neurons do not transduce mechanical stimuli into electrical signals

(A) Schematic illustration of the mechano-clamp technique used to evoke and record mechanically-activated currents.

(B) Representative example traces of whole cell currents (bottom traces) evoked by mechanical stimulation (top traces) in the indicated cell types. Note, CHRNA3^{+} neurons do not exhibit mechanotransduction currents.

(C) The mean ± SEM peak mechanotransduction current amplitudes are shown as a function of membrane displacement.

(D) Comparison of the proportions of mechanoinsensitive (n.r.) and mechanosensitive neurons in the indicated sensory neuron subpopulations.

(E) Overlay of phase-contrast and fluorescence image of an IB4-labelled DRG culture from a CHRNA3-EGFP mouse.

(F) Typical AP of the indicated cell types (top traces). The bottom traces show the first derivative (dV/dt) of the AP, which exhibits two local minima if the AP has the nociceptor-specific hump in the falling phase.

(G) Comparison of the mean (bars) ± SEM (error bars) half-peak durations (HPD) of the APs of the indicated cell types. The scattered symbols show the individual HPD values of

each recorded cell. ***: P<0.001; Kruskal-Wallis one-way ANOVA with Dunn's multiple comparison test.

(H) Size distribution histogram of cultured DRG neurons showing that CHRNA3^{+} neurons have medium cell diameters.

Europe PMC Funders Author Manuscripts

Europe PMC Funders Author Manuscripts

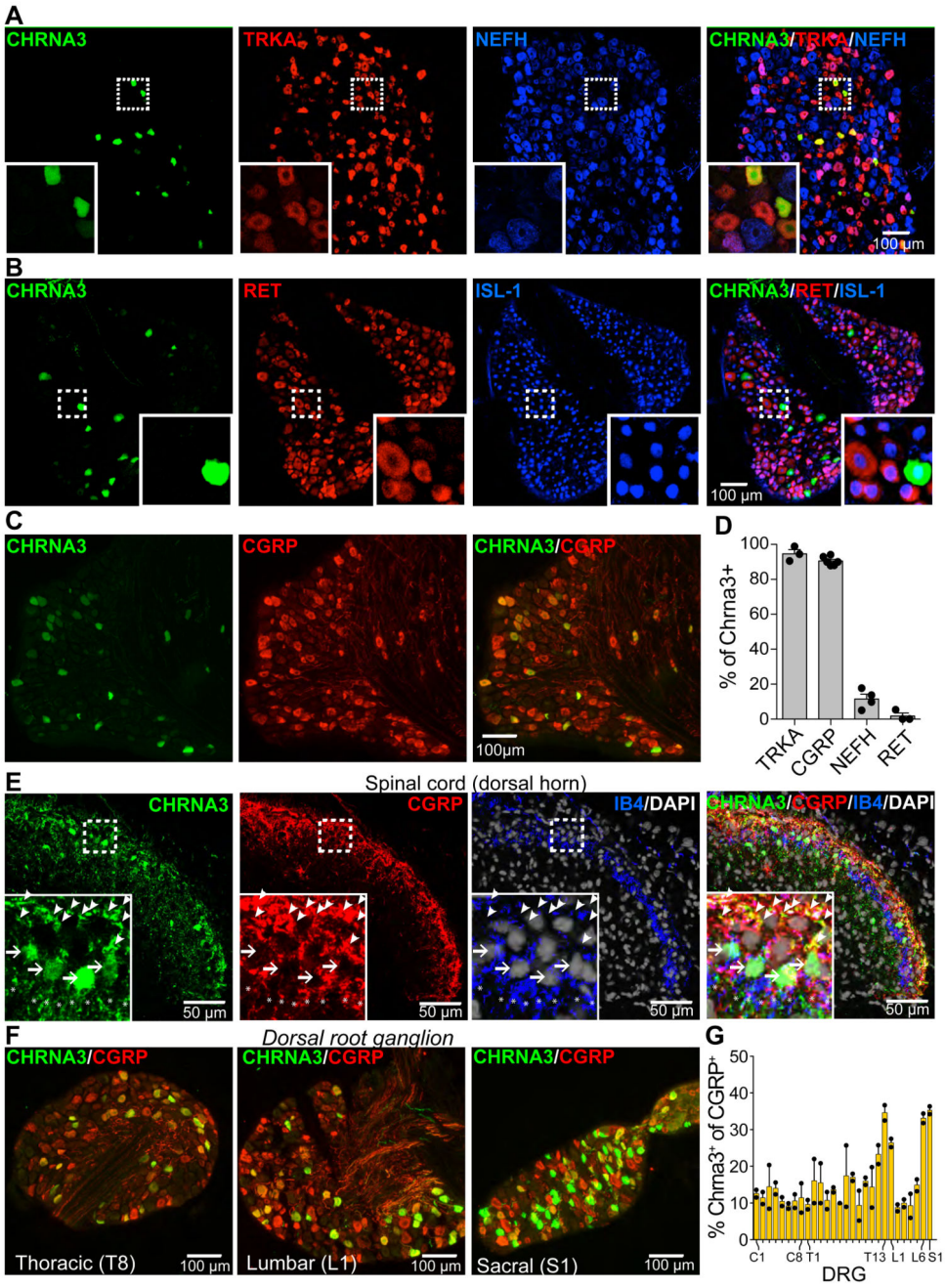

Figure 2. CHRNA3$^+$ neurons are peptidergic C-fiber nociceptors

(A-C) Immunostaining of L3-L5 DRGs showing that CHRNA3+ neurons express the peptidergic nociceptor markers TRKA (A) and CGRP (C) but not NEFH (A) and RET (B).

(D) Mean ± SEM percentage of CHRNA3$^+$ neurons that express the indicated marker protein. (N=3-6 DRGs from 2 different mice; individual data points from each mouse are shown as black circles).

(E) CHRNA3$^+$ fibers project to lamina I of the spinal dorsal horn, which was visualized with CGRP staining. Lamina IIo was visualized by IB4 labeling. CHRNA3$^+$ fibers in lamina II

and below were CGRP-negative (compare signals marked by arrowheads and asterisks in the inset) and hence likely originate from the CHRNA3^{+}/CGRP^{-} local neurons in lamina II (cells marked with arrows).

(F) Representative images showing co-expression of CHRNA3 and CGRP in thoracic (T8, left), lumbar (L1, middle) and sacral (S1, right) DRGs. In sacral DRGs there are numerous neurons with a particularly bright CHRNA3 immunofluorescence signal. For a detailed analysis of the neurochemical and electrophysiological differences between bright and less bright CHRNA3^{+} neurons please see Figure S1 and S2.

(G) Overview of the proportions of CGRP+ neurons that express CHRNA3 in the indicated DRGs (cervical = C, thoracic =T, lumbar =L, sacral = S) Bars represent means ± SEM (N=2 mice, percentage of individual mice are shown as black circles). Note that CHRNA3^{+} are most abundant in thoracolumbar and lumbosacral DRGs.

Europe PMC Funders Author Manuscripts

Europe PMC Funders Author Manuscripts

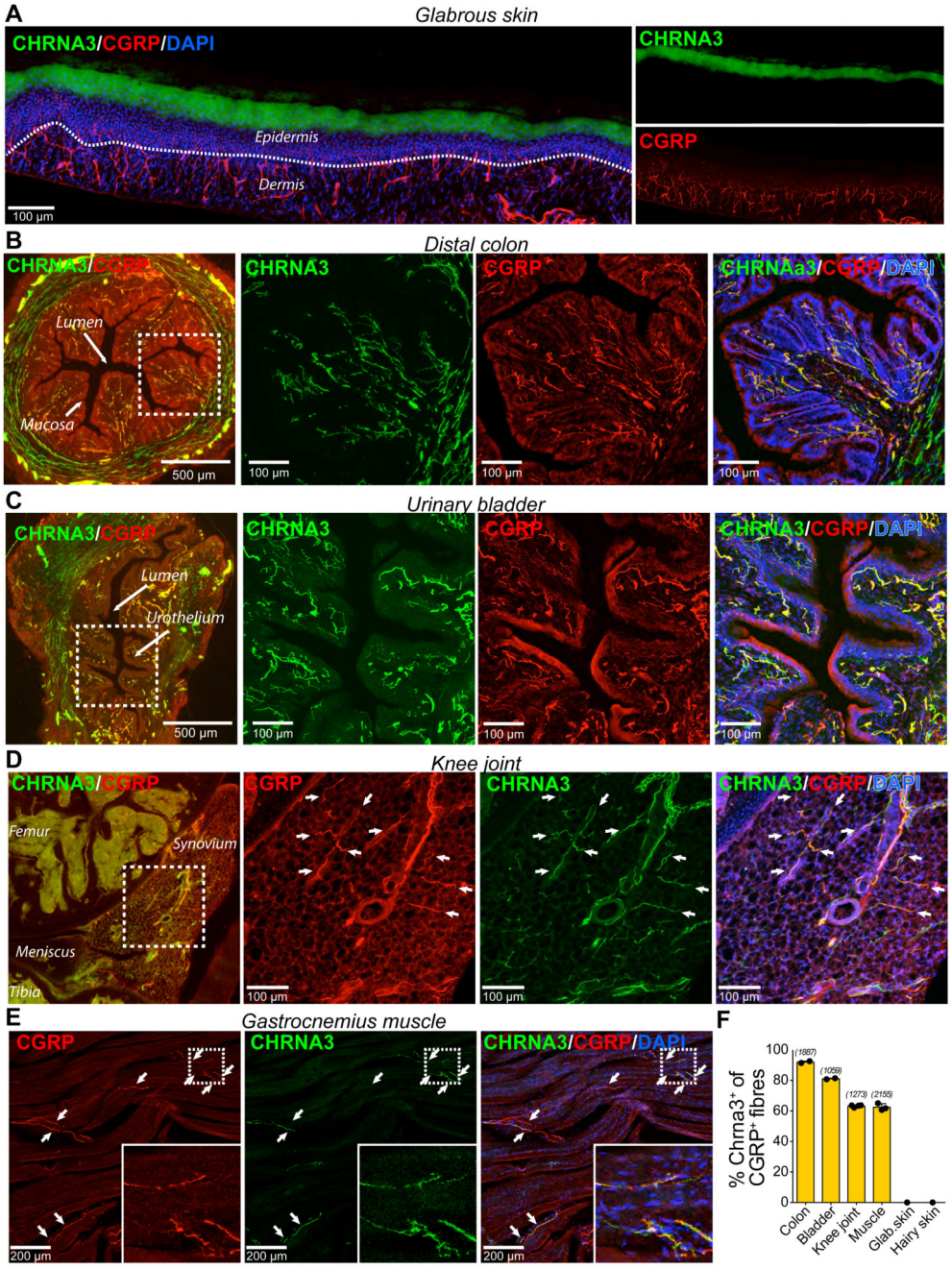

Figure 3. Peripheral projections of CHRNA3^{+} neurons

(A-E) Immunostainings of tissue sections of the glabrous skin (A), the distal colon (B), the urinary bladder (C), the knee joint (D) and the gastrocnemius muscle (E) to visualize innervation by CHRNA3^{+}/CGRP^{+} (green/red) sensory afferents. Also see Figure S3. Images shown in (A) are composite images assembled from multiple high-resolution images. The three images on the right in (B), (C) and (D) show magnified views of the regions marked with the dashed white squares in the leftmost images.

(F) Quantification of the proportion of $CGRP^+$ fibre fragments (i.e. each connected fluorescent entity was considered as a fibre fragment) that express CHRNA3. Bars represent means ± SEM (N=2-4 mice; individual data points from each mouse are shown as black circles).

Europe PMC Funders Author Manuscripts

Europe PMC Funders Author Manuscripts

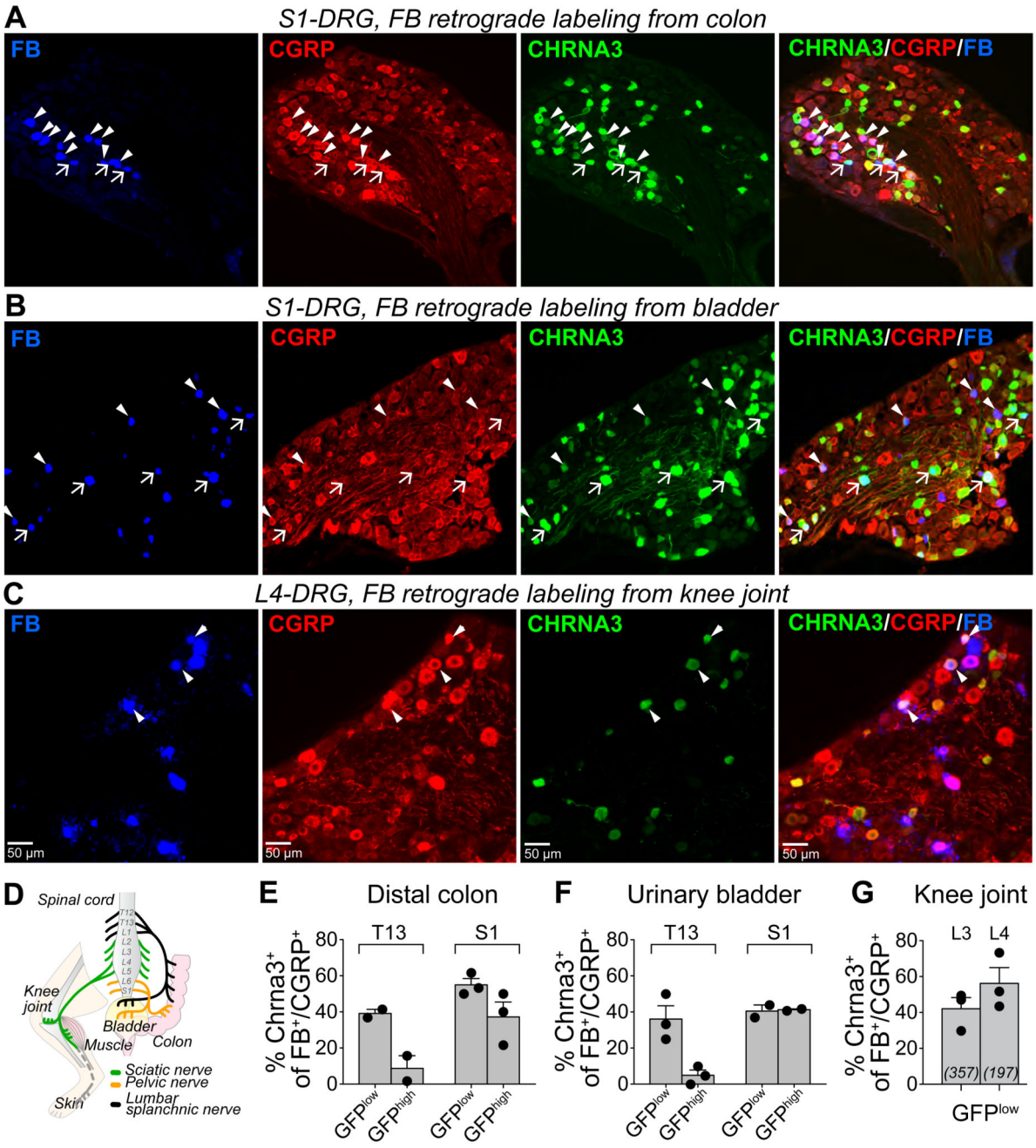

Figure 4. Retrograde labeling of sensory afferents innervating the colon, the bladder and the knee joint.

(A-C) Representative images of DRG neurons retrogradely labeled with Fast Blue (FB) from the colon (A), the bladder (B) and the knee joint (C) and co-stained for CHRNA3 and CGRP. Arrowheads in (A-C) mark GFP^{low}-$CHRNA3^{+}$ neurons and arrows mark GFP^{high}-$CHRNA3^{+}$ neurons.

(D) Schematic illustration of the origin of sensory afferents that innervate the colon, the bladder, the knee joint and the gastrocnemius muscle.

(E-G) Quantification of the percentage of CHRNA3^{+}-GFP^{low} (mechanoinsensitive) and CHRNA3^{+}-GFP^{high} (mechanosensitive) among FB^{+}/CGRP^{+} in T13, S1 and L3-L4 DRGs – i.e. among CGRP^{+} afferents that innervate the colon (E), the bladder (F) and the knee joint (G). Bars represent means ± SEM (N = 2-3 mice; proportions of individual mice are shown as black circles). Note, CHRNA3-GFP^{low} (mechanoinsensitive) afferents account for ~50% of all CGRP+ afferents in the bladder, colon and knee joint.

Europe PMC Funders Author Manuscripts

Europe PMC Funders Author Manuscripts

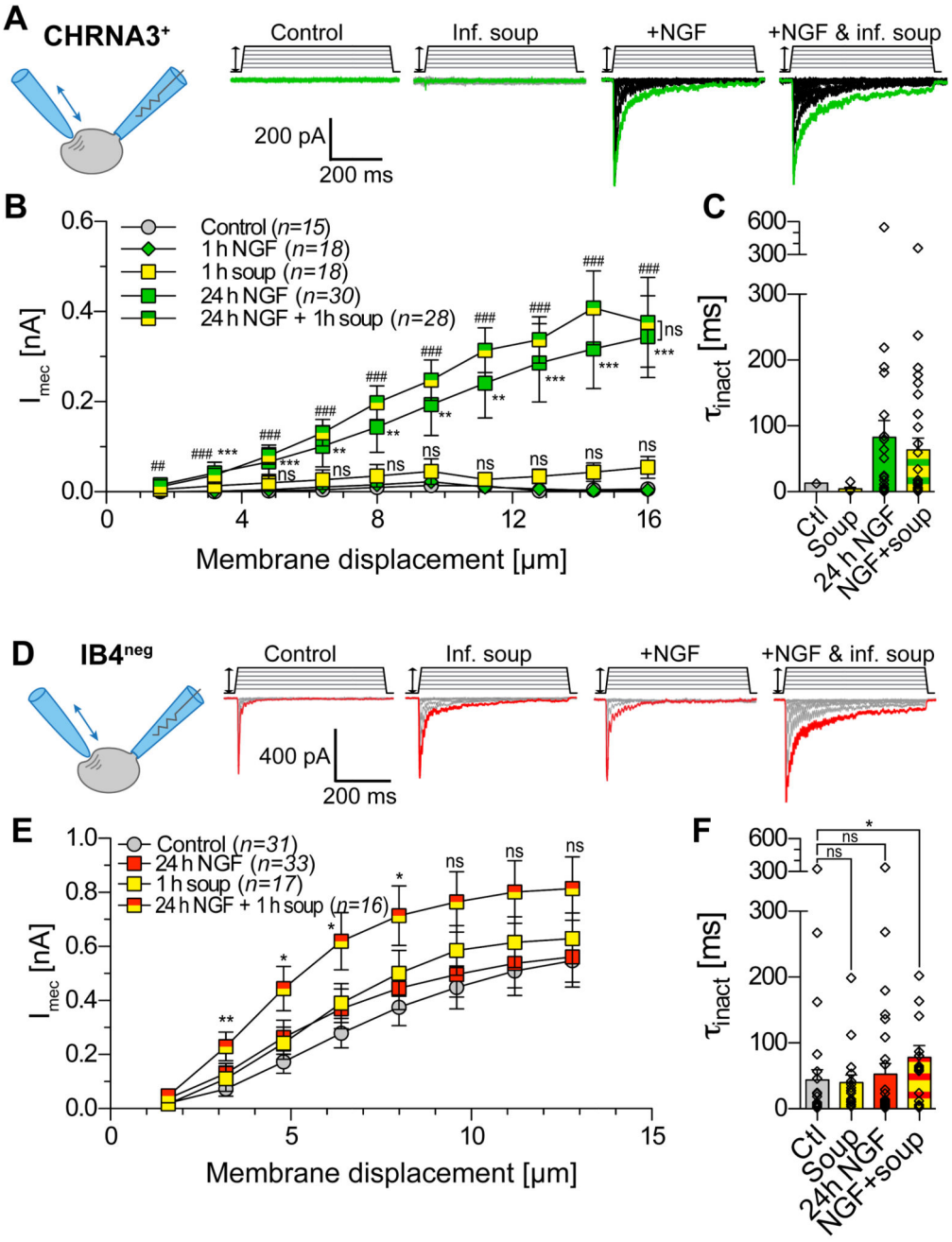

Figure 5. NGF sensitizes CHRNA3^{+} neurons but not IB4^{neg} neurons to mechanical stimuli

(A) Representative example traces of whole cell currents (bottom traces) evoked by mechanical stimulation (top traces) in CHRNA3^{+} neurons cultured for 24 h in normal growth medium (control), for 24 h in growth medium + 1h inflammatory soup before recording (inf. soup), after 24 h treatment with 50 ng/ml NGF (+NGF) and after 24 h NGF + 1 h inflammatory soup.

(B) The mean ± SEM mechanotransduction current amplitudes of CHRNA3^{+} neurons subjected to the indicated treatments are shown as a function of membrane displacement.

Europe PMC Funders Author Manuscripts

CHRNA3^{+} only acquire mechanosensitivity after treatment with NGF. Current amplitudes evoked by the same membrane displacement in the different conditions were compared using Kruskal-Wallis one-way ANOVA and Dunn's multiple comparison test. The P-values of Dunn's multiple comparison test are indicated by asterisks (*) for control vs. 24 h NGF and by a hash (#) for control vs. 24h NGF + 1h soup. (*** and ###, $P < 0.001$; ** and ##, $P < 0.01$; ns = not significant).

(C) Comparison of the inactivation time constants (τ_{inact}) of the mechanotransduction currents recorded in the indicated conditions. Bars represent the mean ± SEM τ_{inact} and the individual data points from which the means were calculated are shown in the aligned dot plot.

(D-F) The panels D-F show the same parameters as the panels A-C, but for mechanotransduction currents evoked in small diameter IB4^{neg} neurons. Note that NGF neither modulates mechanotransduction current amplitudes nor inactivation kinetics.

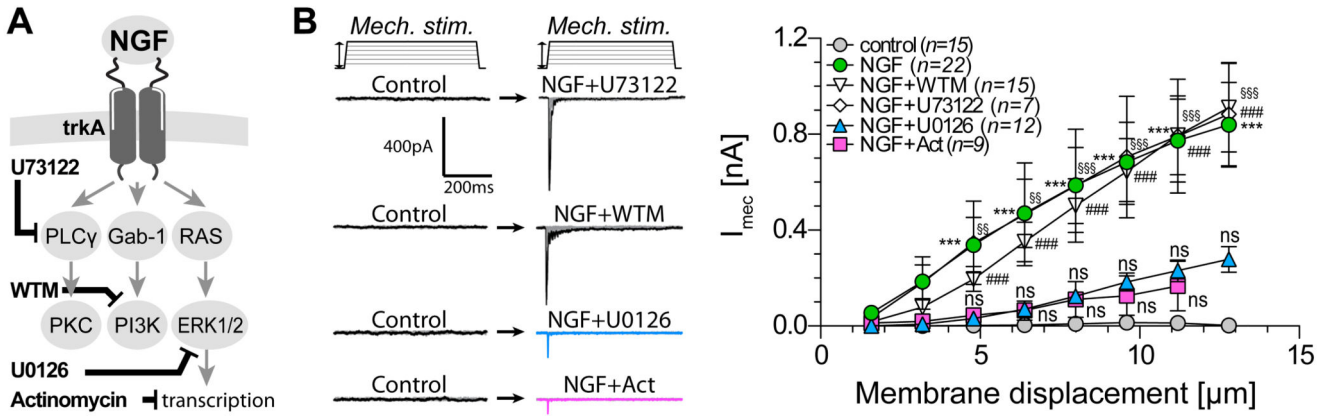

Figure 6. The acquisition of mechanosensitivity requires *de-novo* gene transcription

(A) Schematic illustration of the intracellular signaling cascades activated by NGF.

(B) Example traces (left panel) and displacement-response curves (right panel) of mechanotransduction currents of CHRNA3^{+} neurons treated with NGF and the indicated inhibitors of the signaling cascades shown in (A). Current amplitudes evoked by the same membrane displacement in the different conditions were compared using Kruskal-Wallis one-way ANOVA and Dunn's multiple comparison test. The P-values of Dunn's multiple comparison test are indicated by asterisks (*) for 24 h NGF vs. control, by hashes (#) for NGF + U73122 vs. control and by section signs (§) for NGF + wortmannin vs. control (***, ###, §§§, P < 0.001; **, ##, §§, P < 0.01; ns = not significant).

Europe PMC Funders Author Manuscripts

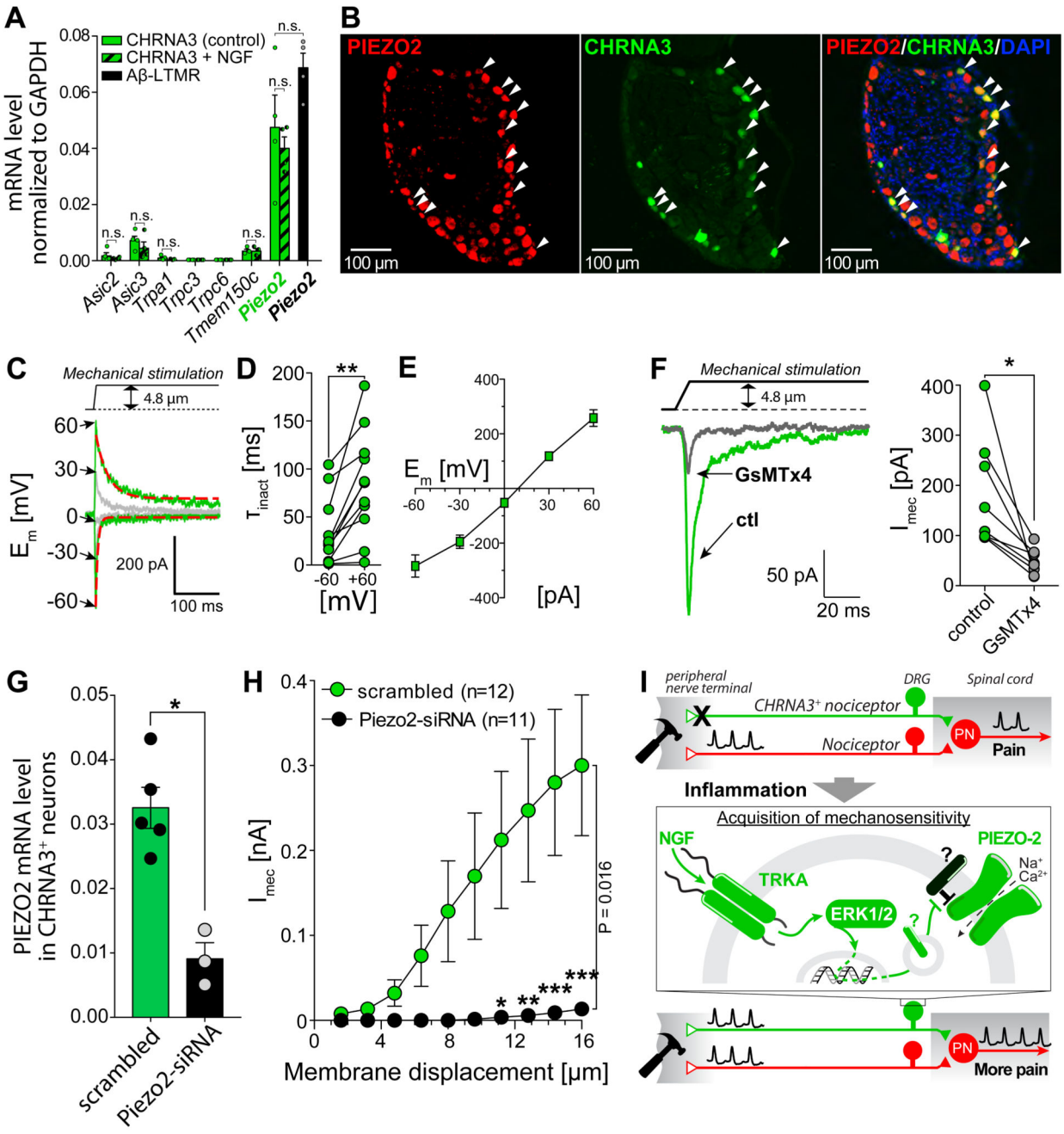

Figure 7. Mechanotransduction in CHRNA3$^+$ neurons requires PIEZO2

(A) Comparison of the expression levels of the indicated genes in CHRNA3$^+$ neurons under control conditions (green bars) and after 24 h treatment with NGF (hatched bars). Note that under control conditions CHRNA3$^+$ neurons express Piezo2 at similar levels as Aβ-LTMRs (black bar), even though they do not exhibit mechanotransduction currents under these conditions. Bars represent mean ± SEM from 3-4 samples (one sample per mouse).

(B) Immunolabeling of an L4 DRG showing PIEZO2 expression in CHRNA3$^+$ neurons (marked by arrowheads).

(C) Example traces of mechanotransduction currents evoked by a 4.8 μm membrane displacement of a CHRNA3$^+$ neuron at the indicated membrane potentials. Inactivation was fitted with a single exponential function (red dashed line).
(D) Paired dot plot comparing inactivation time constants (τ_{inact}) of mechanotransduction currents at -60 mV and +60 mV. At +60 mV currents inactivate significantly slower than at -60 mV (paired T-test, P = 0.0012)
(E) I-V-curve showing that mechanotransduction currents in CHRNA3$^+$ neurons after 24h NGF treatment reverse at around 0 mV, suggesting that they are mediated by a non-selective cation channel. Symbols represent means ± SEM (n=11).
(F) Example traces (left) and paired dot plot (right) showing that mechanotransduction currents in CHRNA3$^+$ neurons are inhibited by GsMTx4 (paired T-test, n = 8, P = 0.0118).
(G) Comparison of the Piezo2 expression levels in CHRNA3+ neurons transfected with not-targeting siRNA (scrambled) and Piezo2-siRNA, showing that Piezo2 expression was reduced by ~72% (0.032 ± 0.0031 vs. 0.0091 ± 0.0025; Mann-Whitney test, P=0.0357).
(H) Comparison of the displacement-response curves of NGF-treated CHRNA3$^+$ neurons transfected with not-targeting siRNA (green circles) and Piezo2-siRNA (black circles). Curves were compared using a two-way repeated measures ANOVA (P = 0.016) with Bonferroni post test (*, P < 0.05; **, P < 0.01; ***, P < 0.001).
(I) Model of the mechanism underlying the acquisition of mechanosensitivity and the possible contribution to increased pain sensitivity during inflammation.

Europe PMC Funders Author Manuscripts